View-based SLAM using Omnidirectional Images

D. Valiente, A. Gil, L. Fernández and O. Reinoso
System Engineering Department, Miguel Hernández University, 03202 Elche (Alicante), Spain

Keywords: Visual SLAM, Omnidirectional Images.

Abstract: In this paper we focus on the problem of Simultaneous Localization and Mapping (SLAM) using visual information obtained from the environment. In particular, we propose the use of a single omnidirectional camera to carry out this task. Many approaches to visual SLAM concentrate on the estimation of the position of a set of 3D points, commonly denoted as visual landmarks which are extracted from images acquired at the environment. Thus the complexity of the map computation grows as the number of visual landmarks in the map increases. In this paper we propose a different representation of the environment that presents a series of advantages compared to the before mentioned approaches, such as a simplified computation of the map and a more compact representation of the environment. Concretely, the map is represented by a set of views captured from particular places in the environment. Each view is composed by its position and orientation in the map and a set of 2D interest points represented in the image reference frame. Thus, in each view the relative orientation of a set of visual landmarks is stored. During the map building stage, the robot captures an image and finds corresponding points between the current view and the views stored in the map. Assuming that a set of corresponding points is found, the transformation between both views can be computed, thus allowing us to build the map and estimate the pose of the robot. In the suggested framework, the problem of finding correspondences between views is troublesome. Consequently, with the aim of performing a more reliable approach, we propose a new method to find correspondences between two omnidirectional images when the relative error between them is modeled by a gaussian distribution which correlates the current error on the map. In order to validate the ideas presented here, we have carried out a series of experiment in a real environment using real data. Experiment results are presented to demonstrate the validity of the proposed solution.

1 INTRODUCTION

The problem of SLAM is of paramount importance in the field of mobile robots, since a model of the environment is often required for navigation purposes. The map building process is complex, since the robot needs to build a map incrementally, while, simultaneously, computing its location inside the map. The computation of a coherent map is problematic, since the sensor data is corrupted with noise that affects the simultaneous estimation of the map and the path followed by the robot.

To the present days, approaches to SLAM can be classified according to the kind of sensor data used to estimate the map, the representation of the map and the basic algorithm used for its computation. For example, due to their precision and robustness, laser range sensors have been used extensively to build maps (Stachniss et al., 2004; Montemerlo et al., 2002). In this sense, two map representations have been typically used: 2D occupancy grid maps with raw laser (Stachniss et al., 2004), and the extraction of features from the laser measurements (Montemerlo et al., 2002) that are used to build 2D landmark-based maps.

A subarea in the SLAM community proposes the utilization of visual information to build the map. These approaches use cameras as the main sensor and, in consequence are usually denoted as visual SLAM. Cameras possess a series of features that make them attractive for its application to the SLAM problem. However, vision sensors are generally less precise than laser sensors and the research focuses on the methods to extract usable information for the SLAM process.

In the latter group, we can find a great variety of camera arrangements. For example, stereo-based approaches in which two calibrated cameras extract 3D relative measurements to a set of visual landmarks, being each landmark accompanied by a visual

Valiente D., Gil A., Fernández L. and Reinoso O..
View-based SLAM using Omnidirectional Images.
DOI: 10.5220/0004031800480057
In *Proceedings of the 9th International Conference on Informatics in Control, Automation and Robotics* (ICINCO-2012), pages 48-57
ISBN: 978-989-8565-22-8

descriptor computed from its visual appearance (Gil et al., 2010b). In this approach a Rao-Blackwellized particle filter is used to estimate the map and path followed by the robots. Other approaches propose the use of a single camera to estimate a map of 3D visual landmarks and the 6 DOF pose of the camera (Davison and Murray, 2002) with an EKF-SLAM algorithm. Each visual landmark is detected with the Harris corner detector (Harris and Stephens, 1988) and described with a grey level patch. Since the distance to the visual landmarks cannot be measured directly with a single camera, the initialization of the 3D coordinates of a landmark poses a problem. This fact inspired the inverse depth parametrization exposed in (Civera et al., 2008). A variation of the Information Filter is used in (Joly and Rives, 2010) to estimate a visual map using a single omnidirectional camera and an inverse depth parametrization of the landmarks. Also, in (Jae-Hean and Myung Jin, 2003) two omnidirectional cameras are combined to obtain a wide field of view stereo vision sensor. In (Scaramuzza, 2011), the computation of the essential matrix between two views allows to extract the relative motion between two camera poses, which leads to a visual odometry. According to (Andrew J. Davison et al., 2004), the performance of the single-camera SLAM is improved when using a wide field of view lens, which suggests the use of an omni-directional camera in visual SLAM, since, in this case, the horizontal field of view is maximum.

The approach presented in this paper assumes that the mobile robot is equipped with a single omnidirectional camera. As shown in Figure 1(a), the optical axis of the camera points upwards, thus a rotation of the robot moving on a plane is equivalent to a shift along the columns of the panoramic image captured.

In this paper a different representation of the environment is proposed. To date, most of the work in visual SLAM dealt with the estimation of the position of a set of visual landmarks expressed in a global reference frame (Davison and Murray, 2002; Gil et al., 2010b; Andrew J. Davison et al., 2004; Civera et al., 2008). In this work, we concentrate on a different representation of the environment: the map is formed by the position and orientation of a set of views in the environment. Each view is composed by an omnidirectional image captured at a particular position, its orientation in the environment and a set of interest points extracted from it. Each interest point is accompanied by a visual descriptor that encodes the visual appearance of the point. With this information stored in the map, we show how the robot is able to build the map and localize inside it. When the robot moves in the neighbourhood of any view stored in the map and captures an image with the camera, a set of interest points will be matched between the current image and the view. Next, a set of correspondences can be found between the images. This information allows us to compute the relative movement between the images. In particular, the rotation between images can be univocally computed, as well as the translation (up to a scale factor). To obtain these measurements between images we rely on a modification of the Seven Point Algorithm (Scaramuzza et al., 2009; Scaramuzza, 2011). This idea is represented in Figure 1(b), where we show two omnidirectional images and some correspondences indicated. The transformation between both reference systems is also shown. The computation of the transformation relies on the existence of a set of corresponding points, thus, when the robot moves away from the position of the stored view, the appearance of the scene will vary and it may be difficult to find any corresponding points. In this case, a new view will be created at the current position of the robot. The new initialized view allows for the localization of the robot around its neighbourhood. It is worth noting that a visual landmark corresponds to a physical point, such as a corner on a wall. However, a view represents the visual information that is obtained from a particular pose in the environment. In this sense, a view is an image captured from a pose in the environment that is associated with a set of 2D points extracted from it. In the experiments we rely on the SURF features (Bay et al., 2006) for the detection and description of the points.

We consider that the map representation introduced here presents some advantages compared to previous visual SLAM approaches. The most important is the compactness of the representation of the environment. For example, in (Civera et al., 2008) an Extended Kalman Filter (EKF) is used to estimate the position of the visual landmarks, as well as the position and orientation of the camera. With this representation each visual landmarks is represented by 6 variables, thus the state vector in the EKF grows rapidly as the number of visual landmarks increases. This fact poses a challenge for most existing SLAM approaches. In opposition with these, in the algorithm presented here, only the pose of a reduced set of views is estimated. Thus, each view encapsulates information of a particular area in the environment, in the form of several interest points detected in the image. Typically, as will be shown in the experiments, a single view may retain a sufficient number of interest points so that the localization in its neighbourhood can be performed.

Storing only a set of views of the environment has, however, some drawbacks. We have to face the prob-

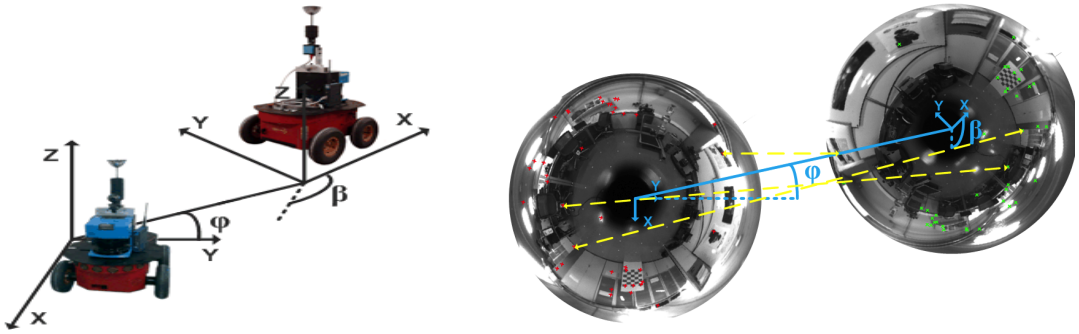

(a) (b)

Figure 1: Figure 1(a) shows the sensor setup used during the experiments. Figure 1(b) presents two real omnidirectional images, with some correspondences indicated and the observation variables ϕ and β.

lem of determining a set of correspondences between two views. Determining a metric transformation between two omnidirectional images is not trivial in the presence of false data associations. However, in Section 3 we present an algorithm that can be used to process images at a fast rate for online SLAM. In this case, the computation of the transformation between two images depends only on the number of matches, that can be easily adjusted to provide both speed and precise results. Moreover we suggest a gaussian propagation of the current error of the map in order to come up with a reliable scheme of matching, so that false correspondences are avoided.

We present a series of experiments and their results obtained trough the acquisition of real omnidirectional images that demonstrate the validity of the approach. The set of experiments have been carried out by varying several parameters of the SLAM filter when using real images captured in an office-like environment. The paper is organized as follows: Section 2 describes the SLAM process using the proposed framework. Next, the algorithm used to estimate the transformation between two omnidirectional images is described in Section 3. Following, Section 4 presents the experimental results. Finally, Section 5 establishes a discussion to analyze the results.

2 SLAM

This section describes in detail the representation of the environment as well as the map building process. As mentioned before, the visual SLAM problem is set out as the estimation of the position and orientation of a set of views. Thus, the map is formed by a set of omnidirectional images obtained from different poses in the environment. In opposition with other solutions, the views do not correspond to any physical landmarks or element in the environment (e.g. a corner, or the trunk of a tree). In our case, a landmark (renamed *view*) will be constituted by an omnidirectional image captured at the pose $x_l = (\mathrm{x}_l, \mathrm{y}_l, \theta_l)$ and a set of interest points extracted from that image.

In our opinion, this map representation can be estimated using different kind of SLAM algorithms, including online methods such as, EKF (Davison and Murray, 2002), Rao-Blackwellized particle filters (Montemerlo et al., 2002) or offline algorithms, such as, for example, Stochastic Gradient Descent (Grisetti et al., 2007). In this paper we present the application of the EKF to the proposed map representation and explain how to obtain correct results using real data.

In addition we consider that the map representation and the measurement model can be also applied using standard cameras. The reason for using omnidirectional images is their ability to acquire a global view of the environment in a single image, due to their large field of view, resulting in a reduced number of variables to represent the map.

2.1 View-based Map

The pose of the mobile robot a time t will be denoted as $x_v = (\mathrm{x}_v, \mathrm{y}_v, \theta_v)^T$. Each view $i \in [1, \ldots, N]$ is constituted by its pose $x_{l_i} = (\mathrm{x}_l, \mathrm{y}_l, \theta_l)_i^T$, its uncertainty P_{l_i} and a set of M interest points p_j expressed in image coordinates. Each point is associated with a visual descriptor d_j, $j = 1, \ldots, M$.

Figure 2 describes this map representation, where the position of several views is indicated. For example, the view A is stored at the pose $x_{l_A} = (\mathrm{x}_{l_A}, \mathrm{y}_{l_A}, \theta_{l_A})^T$ in the map and has a set of M points detected. The view A and C allow for the localization of the robot in the corridor. The view B represents the first room, whereas the view D and E represent the second and third room respectively, and make the robot capable to localize in the environment.

Thus, the augmented state vector is defined as:

$$\bar{x} = \begin{bmatrix} x_v & x_{l_1} & x_{l_2} & \cdots & x_{l_N} \end{bmatrix}^T \quad (1)$$

where $x_v = (\mathrm{x}_v, \mathrm{y}_v, \theta_v)^T$ is the pose of the moving vehicle and $x_{l_N} = (\mathrm{x}_{l_N}, \mathrm{y}_{l_N}, \theta_{l_N})$ is the pose of the N-view that exist in the map.

2.2 Map Building Process

This subsection introduces an example of map building in an indoor environment, represented in Figure 2. We consider that the robot explores the environment while capturing images with its omnidirectional camera. The exploration starts at the origin denoted as A, placed at the corridor. At this time, the robot captures an omnidirectional image I_A, that is stored as a view with pose x_{l_A}. We assume that, when the robot moves inside the corridor, several point correspondences can be found between I_A and the current omnidirectional image. Given this set of correspondences, the robot can be localized with respect to the view I_A. Next, the robot continues with the exploration. When it enters the first room, the appearance of the images vary significantly, thus, no matches are found between the current image and image I_A. In this case, the robot will initiate a new view named I_B at the current robot position that will be used for localization inside the room. Finally, the robot keeps moving through the corridor and goes into different rooms and creates new views respectively at these points. The number of images initiated in the map depends directly on the kind of environment. In the experiments carried out with real data we show that typically, a reduced number of views can be used while obtaining precise results in the computation of the map.

In addition, SLAM algorithms can be classified as online SLAM when they estimate the map and the pose x_v at time t. Other algorithms solve the full SLAM problem and estimate the map and the path of the robot until time t, $x_{1:t} = [x_{v_1}, x_{v_2}, \ldots, x_{v_t}]$. The EKF is generally classified in the first group, since, at each time t the filter gives an estimation of the current pose x_v. However, in our case, the position of the view i coincides with the pose of the robot at any of the views. In consequence the EKF filter allows to compute the pose of the robot at time t and, in addition, a subset of the path followed by the vehicle formed by the poses $x_v, x_{l_1}, x_{l_2}, x_{l_N}$.

2.3 Observation Model

Following, the observation model is described. We consider that we have obtained two different omnidirectional images captured at two different poses in the environment. One of the images is stored in the map and the other is the current image captured by the robot at the pose x_v. We assume that given two images we are able to extract a set of significant points in both images and obtain a set of correspondences. Next, as will be described in Section 3, we are able to obtain the observation z_t:

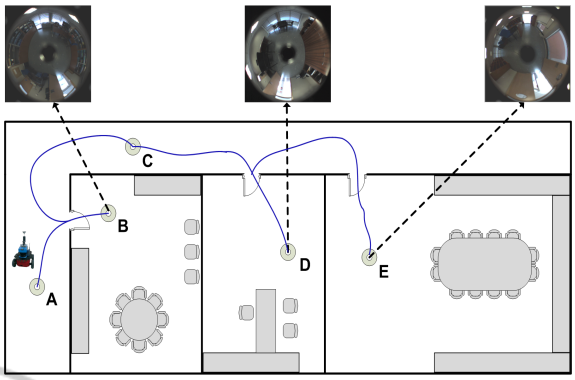

Figure 2: Main idea for map building. The robot starts the exploration from A by storing a view I_A. While the robot moves and no matches are found between the current image and I_A, a new view is created at the current position of the robot, for instance in B. The process continues until the whole environment is represented

$$z_t = \begin{pmatrix} \phi \\ \beta \end{pmatrix} = \begin{pmatrix} \arctan\left(\frac{\mathrm{y}_{l_N} - \mathrm{y}_v}{\mathrm{x}_{l_N} - \mathrm{x}_v}\right) - \theta_v \\ \theta_{l_N} - \theta_v \end{pmatrix} \quad (2)$$

where the angle ϕ is the bearing at which the view N is observed and β is the relative orientation between the images. The view N is represented by $x_{l_N} = (\mathrm{x}_{l_N}, \mathrm{y}_{l_N}, \theta_{l_N})$, whereas the pose of the robot is described as $x_v = (\mathrm{x}_v, \mathrm{y}_v, \theta_v)$. Both measurements (ϕ, β) are represented in Figure 1(a).

2.4 Initializing New Views in the Map

We propose a method to add new views in the map when the appearance of the current view differs significantly from any other view existing in the map. A new omnidirectional image is stored in the map when the number of matches found in the neighbouring views is low. Concretely, we use the following ratio:

$$R = \frac{2m}{n_A + n_B} \quad (3)$$

that computes the similarity between views A and B, being m the total number of matches between A and B and n_A and n_B the number of detected points in images A and B respectively. The robot includes a new view in the map if the ratio R drops below a pre-defined threshold. To initialize a new view, the pose of the view is obtained from the current estimation of the

robot pose and its uncertainty equals the uncertainty in the pose of the robot.

3 COMPUTING A TRANSFORMATION BETWEEN OMNI-DIRECTIONAL IMAGES

In this section we present the procedure to retrieve the relative angles β and ϕ between two omni-directional images, as represented in Figure 1(b). As shown before, these angles compose the observation described in (2). Computing the observation involves different problems: first, the detection of feature points in both images and next, finding a set of point correspondences between images that will be used to recover a certain camera rotation and translation. Traditional schemes, such as (Kawanishi et al., 2008; Nister, 2003; Stewenius et al., 2006) apply epipolar constrains between both images and solve the problem in the general 6 DOF case, whereas in our case, according to the specific motion of the robot on a plane, we reduce the problem to the estimation of 3DOF.

3.1 Detection of Interest Points

SURF features (Bay et al., 2006) are used to find interest points in the images and to describe their visual appearance. In (Gil et al., 2010a), SURF features outperform other detectors and descriptors in terms of robustness of the detected points and invariance of the descriptor. SURF features have been previously used in the context of localization (Murillo et al., 2007) using omnidirectional images. We transform the omnidirectional images into a panoramic view in order to increase the number of valid matches between images due to the lower appearance variation obtained with this view.

3.2 Matching of Interest Points

In order to obtain a set of reliable correspondences between two views, several restrictions have to be considered. Some authors (Scaramuzza, 2011) rely on the epipolar geometry to restrict the search of correspondences. The same point detected in two images can be expressed as $p = [x,y,z]^T$ in the first camera reference system and $p' = [x',y',z']^T$ in the second camera reference system. Then, the epipolar condition establishes the relationship between two 3D points p and p' seen from different views.

$$p'^T E p = 0 \tag{4}$$

where the matrix E is denoted as the essential matrix which can be computed from a set of corresponding points in two images.

$$E = \begin{bmatrix} 0 & 0 & \sin(\phi) \\ 0 & 0 & -\cos(\phi) \\ \sin(\beta-\phi) & \cos(\beta-\phi) & 0 \end{bmatrix} \tag{5}$$

being ϕ and β the relatives angles that define a planar motion between two different views, as shown in Figure 1 and (2).

The epipolar restriction (4) has been previously used to compute a visual odometry from two consecutive views (Scaramuzza, 2011), together with some techniques such as *RANSAC* and *Histogram voting* to reject false correspondences. In this sense, the computation of the whole set of detected points is needed in order to find those which satisfy the restriction. Moreover, in the context of visual odometry, consecutive images are close enough to disregard high errors in the pose from where images were taken, so that the epipolar restriction can be normally applied. However, focusing on a SLAM framework, there exists uncertainties in the pose of the robot as well as in the pose of the views that compose the map. For this reason, we consider that is necessary to propagate this errors to accomplish a reliable data association. We suggest using the predicted state vector extracted from the Kalman filter, from which we are able to obtain a predicted observation measurement $\hat{z}_t$ by means of (2). In order to reduce the search of valid corresponding points between images, the map uncertainties have also to be taken into account, so we propagate them to (4) by introducing a dynamic threshold, δ. In a idealistic case, the epipolar restriction may equal to a fixed threshold, meaning that the epipolar curve between images always presents a little static deviation. On a realistic SLAM approach, we should consider that this threshold depends on the existing error on the map, which dynamically varies at each step of the SLAM algorithm. Since this error is correlated with the error on $\hat{z}_t$, we rename δ as $\delta(\hat{z}_t)$. In addition, it has to be noted that (5) is defined up to a scale factor, which is another reason to consider $\delta(\hat{z}_t)$ as a variable value. As a consequence, given two corresponding points between images, they must satisfy:

$$p'^T \hat{E} p < \delta(\hat{z}_t) \tag{6}$$

This approach allows us to reduce the search for corresponding points between images. Figure (3) depicts the procedure. Assuming a detected point $P(x,y,z)$, it may be represented in the first image reference system by a normalized vector $\vec{p}_1$ due to the unknown scale. To deal with this scale ambiguity, we suggest a generation of a point distribution to get a

set of multi-scale points $\lambda_i \vec{p}_1$ for $\vec{p}_1$. This distribution considers a valid range for λ_i according to the predicted $\hat{\rho}$. Please note that the error of the current estimation of the map has to be propagated along the procedure. According to Kalman filter theory, the innovation is defined as the difference between the predicted $\hat{z}_t$ and the real z_t observation measurement:

$$v_i(k+1) = z_i(k+1) - \hat{z}_i(k+1|k) \quad (7)$$

and the covariance of the innovation:

$$S_i(k+1) = H_i(k)P(k+1|k)H_i^T(k) + R_i(k+1) \quad (8)$$

where $H_i(k)$ relates $\bar{x}(k)$ and $z_i(k)$, $P(k+1|k)$ is a covariance matrix that expresses the uncertainty on the estimation, and $R(k)$ is the covariance of the gaussian noise introduced in the process. In addition, $S_i(k+1)$ presents the following structure:

$$S_i(k+1) = \begin{bmatrix} {\sigma_\phi}^2 & \sigma_{\phi\beta} \\ \sigma_{\beta\phi} & {\sigma_\beta}^2 \end{bmatrix} \quad (9)$$

Next, since the predicted $\hat{E}$ can be decomposed in a rotation $\hat{R}$ and a translation $\hat{T}$, we can transform the distribution $\lambda_i \vec{p}_1$ into the second image reference system, obtaining $\vec{q}'_i$. In order to propagate the error, we make use of (9) to redefine the transformation through normal distributions, being $R \sim \mathrm{N}(\hat{\beta}, \sigma_\beta)$ and $T \sim \mathrm{N}(\hat{\phi}, \sigma_\phi)$. This fact implies that $\vec{q}'_i$ is a gaussian distribution correlated with the current map uncertainty. Once obtained $\vec{q}'_i$, they are projected into the image plane of the second image, seen as crossed points in Figure 4. This projection of the normal multi-scale distribution defines a predicted area in the omnidirectional image which is drawn in continuous curve line. This area establishes the specific image pixels where correspondences for $\vec{p}_1$ must be searched for. The shape of this area depends on the error of the prediction, which is directly correlated with the current uncertainty of the map estimation. Dash lines represent the possible candidate points located in the predicted area. Therefore, the problem of matching is reduced to finding the correct corresponding point for $\vec{p}_1$ from those candidates inside the predicted area by comparing their visual descriptor, instead of searching for them at the whole image.

3.3 Computing the Transformation

Once a set of interest SURF points have been detected and matched in two images it is necessary to retrieve the relative angles β and ϕ. In the previous subsection was introduced the term $\hat{E}$ for a predicted matrix to find valid correspondences. Now this set of corresponding points is known, the real E can be determined by directly solving (4). The essential matrix

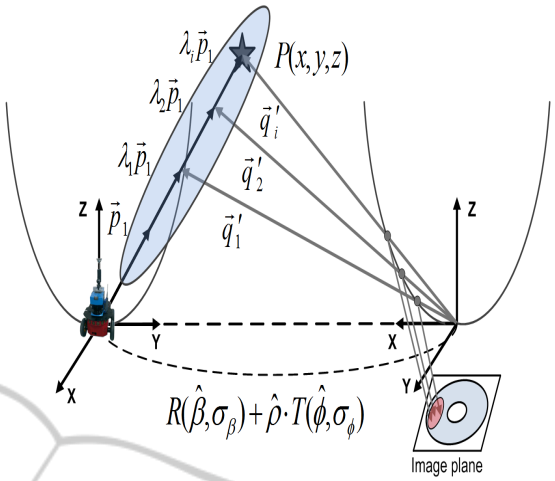

Figure 3: Given a detected point $\vec{p}_1$ in the first image reference system, a point distribution is generated to obtain a set of multi-scale points $\lambda_i \vec{p}_1$. By using the Kalman prediction, they can be transform to $\vec{q}'_i$ in the second image reference system through $R \sim \mathrm{N}(\hat{\beta}, \sigma_\beta)$, $T \sim \mathrm{N}(\hat{\phi}, \sigma_\phi)$ and $\hat{\rho}$. Finally $\vec{q}'_i$ are projected into the image plane to determine a restricted area where correspondences have to be found.

can be expressed as a specific rotation R and a translation T (up to a scale factor), where $E = R \cdot T_x$. The use of a SVD decomposition makes able to retrieve R and T. Following (Bunschoten and Krose, 2003; Hartley and Zisserman, 2004) we obtain the relative angles β and ϕ that define a planar motion between images acquired from different poses. It is worth noting that the motion is restricted to the XY plane, thus only $N = 4$ correspondences are sufficient to solve the problem. Nevertheless we use higher number of correspondences in order to get accurate solutions. Notice that now an external algorithm is not necessary to reject false correspondences since we avoid them through the restricted matching process, limited to specific image area as recently explained.

4 RESULTS

We present three diferent experimental sets. Section 4.1 firstly presents SLAM results to verify the validity of this proposed approach of SLAM. In addition, it presents map building results when varying the number of views that generate the map in order to extract conclusions in the sense of the compactness of the representation. Finally, we present results of accuracy in the obtained map, use of computational resources and their variation with the number of views that conform the map. To carry out these experiments an indoor robot Pioneer P3-AT has been used, which is equipped with a firewire 1280x960

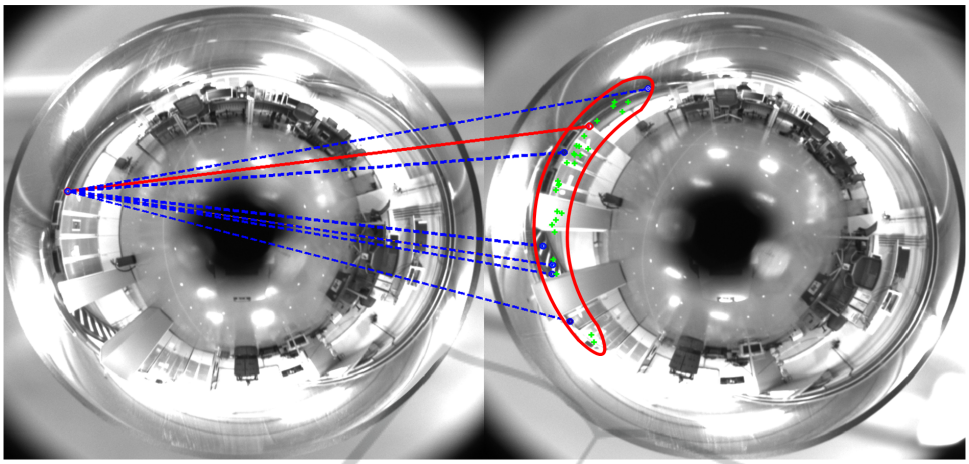

Figure 4: Correspondences for a specific point in the first image are searched for in the predicted area, which is projected into the second image. Crossed points represent the projection of the normal point distribution for the multi-scale points that determine this area. Dash lines show the candidate points in the second image which are inside the predicted area. Continue line represents the correct correspondence for a certain point in the first image. Curve continue line shows the shape of the predicted area.

camera and a hyperbolic mirror. The optical axis of the camera is installed approximately perpendicular to the ground plane, as described in Figure 1(a), in consequence, a rotation of the robot corresponds to a rotation of the image with respect to its central point. Besides, in order to obtain a reference for comparison we use a SICK LMS range finder to generate a ground truth (Stachniss et al., 2004) which provides a resolution of 1m in position.

4.1 SLAM with Real Data

This section presents SLAM results of map building to validate the proposed approach. The robot is guided through an office-like environment of 32x35m while it acquires omnidirectional images and laser range data along the trajectory. Laser data is only used to generate a ground truth for comparison. The robot initiates the SLAM process by adding the first view of the map at the origin, as indicated in Figure 5(a). Next, it keeps on moving along the trajectory while capturing omnidirectional images. The image at the current robot pose is compared to the view in the map looking for corresponding points in order to extract a relative measurement of its position as explained in Section 3. The evaluation of the similarity ratio (3) is also computed, and in case this ratio drops below $R < 0.5$, a new view is initialized at the current robot position with an error ellipse. While the mapping continues, the current image is still being compared with the rest of the views in the map. Figure 5(a) shows the entire process where the robot finishes the navigation going back to the origin. The dash-dotted line represents the solution obtained by the proposed approach, indicating with crosses the points along the trajectory where the robot decided to initiate new views in the map and their uncertainty with error ellipses. The continue line represents the ground truth whereas the odometry is drawn with dash line. As it can be observed, a map for an environment of 32x35m is formed by a reduced set of N=9 views, thus leading to a compact representation. Figure 5(b) compares the errors for the estimated trajectory, the ground truth and the odometry at every step of the trajectory. The validity of the solution is confirmed due to the accomplishment of the convergence required by every SLAM scheme, since the solution error is inside the 2σ interval whereas the odometry error grows out of bounds.

Once the proposed approach was validated, the following experiments were carried out with the aim of testing the compactness of the representation of the environment. Another office-like environment of 42x32m was chosen. In this case the threshold for the similarity ratio R were varied in order to get different map representation for the same environment, in terms of the number of views N that compose the map. The procedure to build up the map follows the steps detailed in the first experiment, and is depicted in Figure 6. Figures 6(a), 6(c), 6(e) show different map versions for this environment with N=7, N=12 and N=20 views respectively. Again, the estimated solution is drawn in dash-dotted line, the odometry in dash line, meanwhile the ground truth in continuous line. View's position are indicated with crosses and their uncertainty with error ellipses. Figures 6(b), 6(d), 6(f), present the errors of the estimated solution and the odometry versus 2σ intervals

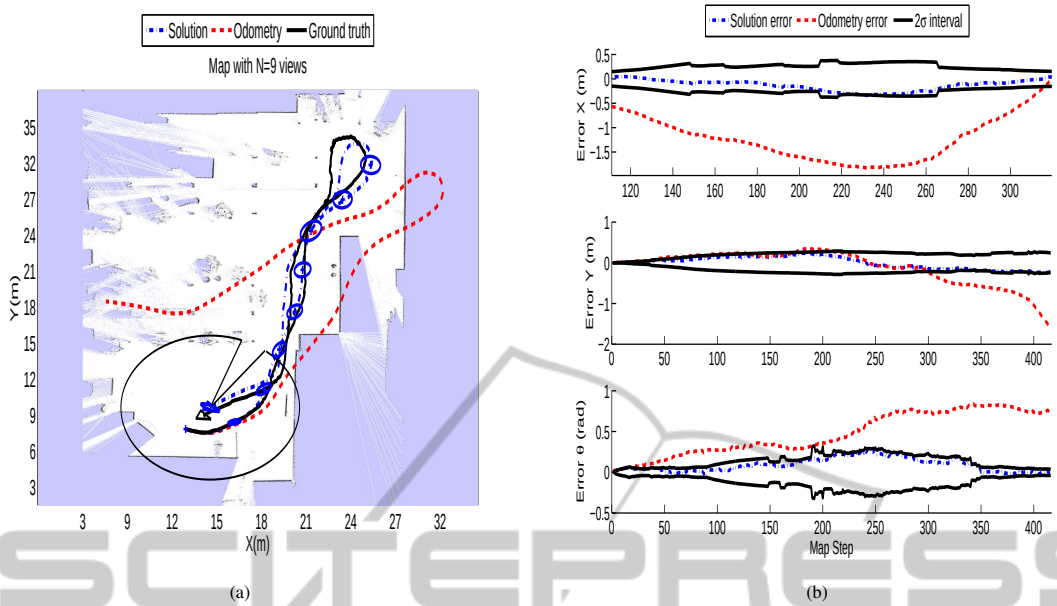

Figure 5: Figure 5(a) presents results of SLAM using real data. The final map is determined by N=9 views, which their positions are represented with crosses and error ellipses. A laser-based occupancy map has been overlapped to compare with the real shape of the environment. Figure 5(b) presents the solution and odometry error in X, Y and θ at each time step.

to test the convergence and validity of the approach for each N-view map. All three estimations satisfy the error requirements for the convergence of the SLAM method, since the solution error is inside the 2σ interval, however the odometry tends to diverge without limit. According to this results, it should be noticed that the higher values of N the lower resulting error in the map. Nevertheless, with the lower value N=7 views, the resulting error is suitable to work in a realistic SLAM problem in robotics. This fact reveals the compactness of the representation. In some context a compromise solution might be adopted when choosing between N, error and obviously computational cost. Next paragraph analysis this issue.

The concept of compactness in the representation of the map has been comfirmed by the previous results. It has been observed that lower values of N provide good results in terms of error. In addition more experiments to obtain maps with different number of views N have been carried out. The results allow us to analyze the computational cost in terms of the number of views N composing the map. In Figure 7 we present these results, showing the RMS error in position and the time consumption, which reveal that the error decreases when N increases. Consequently, the accuracy of the estimation is higher since more views are observed, however the computational cost grows. That is the reason why a compromise solution has to be reached. Generally, SLAM algorithms are real-time intended, so that the time is a limiting factor. Despite this fact, the approach presented here provides accurate results even using a reduced set of views, which is a benefit to consider when there is a lack of computational resources.

5 CONCLUSIONS

In this paper it has been presented an approach to the Simultaneous Localization and Mapping (SLAM) problem using a single omnidirectional camera as a visual sensor. We suggest a different representation of the environment. In contrast to traditional 3D pose estimation SLAM schemes, we only estimate the pose and orientation of a set of omnidirectional images, renamed *views*, as part of the map. A set of interest points described by visual descriptors are associated to each omnidirectional image so that a compact description of the environment is accomplished. Each omnidirectional image allows the robot to compute its localization in the image surroundings. A new matching method is suggested to deal with the problem of finding correspondences. Given two omnidirectional images an a set of interest points for each one, we model the relative error between them by means of a gaussian distribution that correlates the current estimation error on the map to help us to compute a more reliable transformation between images, composed by a rotation and a translation (up to a scale factor). This transformation allows to propose an observation model and to compute a trajectory over a

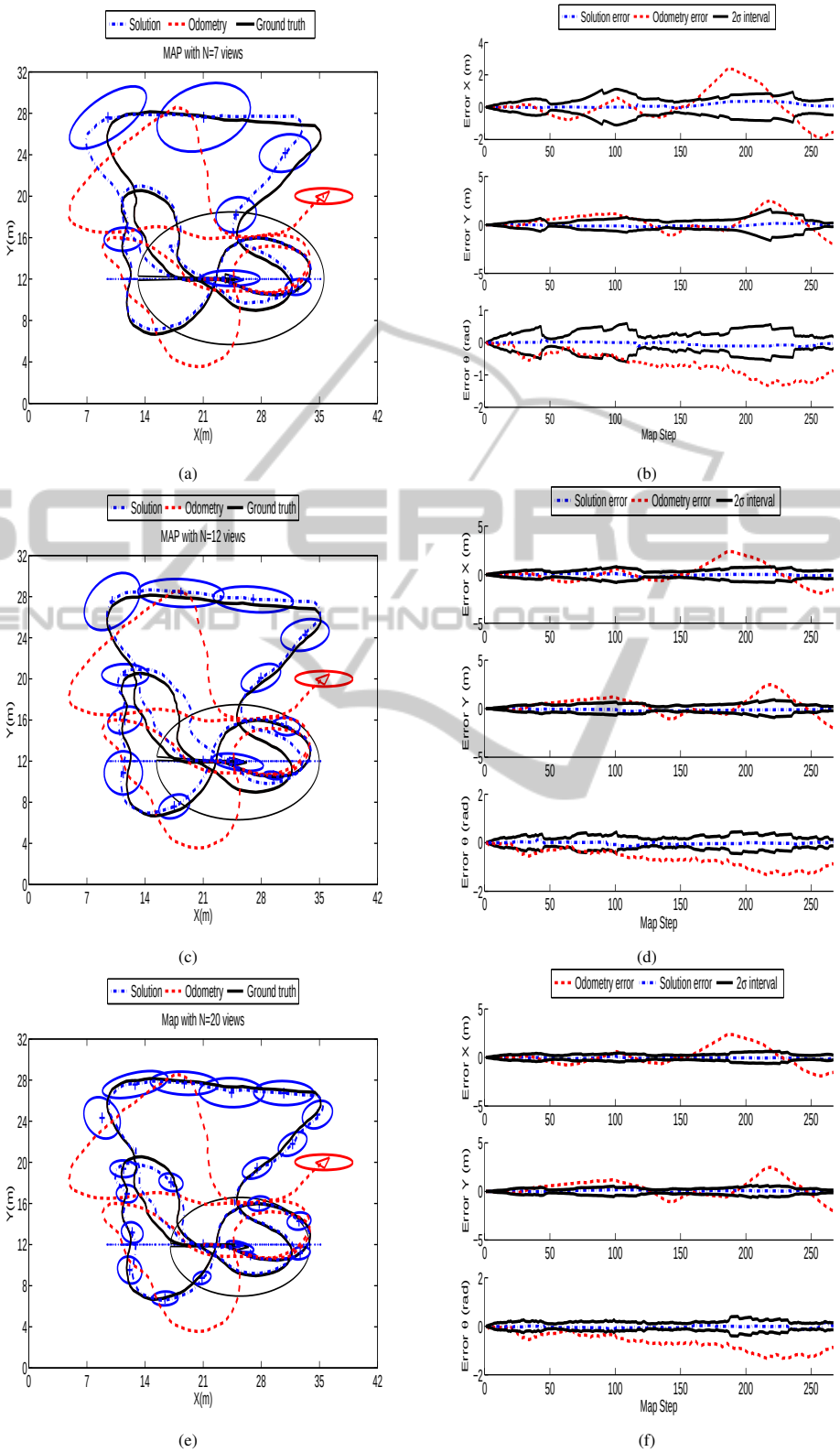

Figure 6: Figures 6(a), 6(c), 6(e) present results of SLAM using real data obtaining different map representations of the environment, formed by N=7, N=12 and N=20 views respectively. The position of the views is presented with error ellipses. Figures 6(b), 6(d), 6(f), present the solution and odometry error in X, Y and θ at each time step for each N-view map.

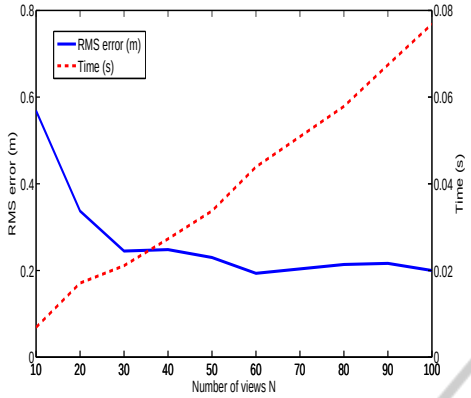

Figure 7: RMS error (m) and time consumption (s) versus the number of views N observed by the robot to compute its pose inside different N-view maps.

map. We append map building results using an EKF-based SLAM algorithm with real data acquisition using an indoor robot, to validate the SLAM approach. In addition we have shown the compactness of the environment representation by building maps with different number of views. Finally we presented a set of measurements to test the accuracy of the solution and the time consumption as a function of the number of views that conform the map.

ACKNOWLEDGEMENTS

This work has been supported by the Spanish government through the project DPI2010-15308.

REFERENCES

Andrew J. Davison, A. J., Gonzalez Cid, Y., and Kita, N. (2004). Improving data association in vision-based SLAM. In *Proc. of IFAC/EURON*, Lisboa, Portugal.

Bay, H., Tuytelaars, T., and Van Gool, L. (2006). SURF: Speeded up robust features. In *Proc. of the ECCV*, Graz, Austria.

Bunschoten, R. and Krose, B. (2003). Visual odometry from an omnidirectional vision system. In *Proc. of the ICRA*, Taipei, Taiwan.

Civera, J., Davison, A. J., and Martínez Montiel, J. M. (2008). Inverse depth parametrization for monocular slam. *IEEE Trans. on Robotics*.

Davison, A. J. and Murray, D. W. (2002). Simultaneous localisation and map-building using active vision. *IEEE Trans. on PAMI*.

Gil, A., Martinez-Mozos, O., Ballesta, M., and Reinoso, O. (2010a). A comparative evaluation of interest point detectors and local descriptors for visual SLAM. *Machine Vision and Applications*.

Gil, A., Reinoso, O., Ballesta, M., Juliá, M., and Payá, L. (2010b). Estimation of visual maps with a robot network equipped with vision sensors. *Sensors*.

Grisetti, G., Stachniss, C., Grzonka, S., and Burgard, W. (2007). A tree parameterization for efficiently computing maximum likelihood maps using gradient descent. In *Proc. of RSS*, Atlanta, Georgia.

Harris, C. G. and Stephens, M. (1988). A combined corner and edge detector. In *Proc. of Alvey Vision Conference*, Manchester, UK.

Hartley, R. and Zisserman, A. (2004). *Multiple View Geometry in Computer Vision*. Cambridge University Press.

Jae-Hean, K. and Myung Jin, C. (2003). Slam with omnidirectional stereo vision sensor. In *Proc. of the IROS*, Las Vegas (Nevada).

Joly, C. and Rives, P. (2010). Bearing-only SAM using a minimal inverse depth parametrization. In *Proc. of ICINCO*, Funchal, Madeira (Portugal).

Kawanishi, R., Yamashita, A., and Kaneko, T. (2008). Construction of 3D environment model from an omnidirectional image sequence. In *Proc. of the Asia International Symposium on Mechatronics 2008*, Sapporo, Japan.

Montemerlo, M., Thrun, S., Koller, D., and Wegbreit, B. (2002). FastSLAM: a factored solution to the simultaneous localization and mapping problem. In *Proc. of the 18th national conference on Artificial Intelligence*, Edmonton, Canada.

Murillo, A. C., Guerrero, J. J., and Sagüés, C. (2007). SURF features for efficient robot localization with omnidirectional images. In *Proc. of the ICRA*, San Diego, USA.

Nister, D. (2003). An efcient solution to the five-point relative pose problem. In *Proc. of the IEEE CVPR*, Madison, USA.

Scaramuzza, D. (2011). Performance evaluation of 1-point RANSAC visual odometry. *Journal of Field Robotics*.

Scaramuzza, D., Fraundorfer, F., and Siegwart, R. (2009). Real-time monocular visual odometry for on-road vehicles with 1-point RANSAC. In *Proc. of the ICRA*, Kobe, Japan.

Stachniss, C., Grisetti, G., Haehnel, D., and Burgard, W. (2004). Improved Rao-Blackwellized mapping by adaptive sampling and active loop-closure. In *Proc. of the SOAVE*, Ilmenau, Germany.

Stewenius, H., Engels, C., and Nister, D. (2006). Recent developments on direct relative orientation. *ISPRS Journal of Photogrammetry and Remote Sensing*.